Porous coating by vacuum plasma spraying on ceramics hip resurfacing implant

C Voisard¹, S Berner¹, C Halewood², P Gruner¹

¹ Medicoat AG, Mägenwil, CH. ² Embody Orthopaedic Ltd, London UK

INTRODUCTION: Clinical complications following metallic ions release from metal-onmetal hip resurfacing implants has led to an early reduction in the deployment of this type of material combination [1]. The need for low wear material pairing and large diameter implants for lower dislocation risks remains though and drives development of alternative solutions like ceramicson-ceramics bearings and full ceramics implants. Coating the ceramic liner suppresses indeed the need of a metallic case (cup) and allows larger ceramics design. In this study a new coating process of titanium and hydroxyapatite using vacuum plasma spraying (VPS) has specifically developed for a high strength zirconiatoughened alumina (BIOLOXdelta CeramTec, Plochingen Germany) and applied to a new resurfacing full ceramics design [2].

METHODS: A rough and porous titanium coating subsequently covered by a hydroxyapatite (HA) coating has been applied to a new resurfacing ceramics prosthesis consisting of a femoral head and an acetabular cup, both made of BIOLOXdelta ceramics [2]. The titanium layer was directly coated on the smooth ceramic surface. Conventional grit blasting process of the surface has been prevented to avoid reduction in fracture strength. Furthermore, a pull off test [3] was developed to assess the adhesion strength directly on the implant surface in addition to the tests required by the international standards [4] like adhesion strength [5], biaxial flexural strength [6] performed with flat coupons.

RESULTS: Biaxial flexure strength of the ceramics substrate of 773 MPa as measured on test coupons is not significantly reduced by the VPS coating process. Nor is the static adhesion tensile strength of 86 MPa influenced by the ceramics surface preparation, as measured on various surfaces (as-fired, milled, ground and polished). Autoclave heat treatment to simulate hydrothermal aging and immersion in Ringer solution slightly

reduced the adhesion strength to values in the order of 75 MPa but without reaching the critical value of 22 MPa [4]. The coating adhesion strength could be verified directly on implants with the local pull out test.

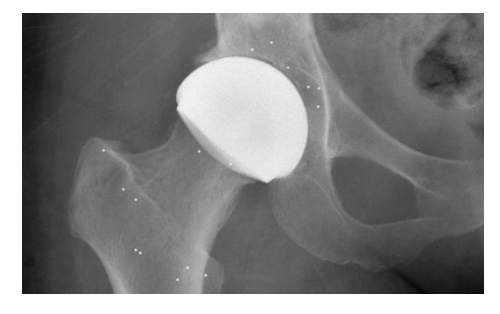


Fig. 1: Post Op X-Ray of H1 resurfacing system (Courtesy Embody Orthopaedics Ltd.).

DISCUSSION & CONCLUSIONS: Both ascoated and aged coatings have been tested and high adhesion strengths could be demonstrated under various conditions, well above the minimum value of 22 MPa defined by various international standards. The novelty of this process is that the implants are not grit blasted and thus the integrity of the ceramics could be preserved as demonstrated with biaxial flexure strength.

REFERENCES: ¹ Sershon et al (2016) Curr Rev Musculoskelet Med 9(1):84-92. ² Multicentre Observational Study Evaluating the Clinical Outcome of the H1 Ceramic Hip Resurfacing Arthroplasty (H1HRA), ClinicalTrials.gov NCT03326804. ³ ASTM Identifier: D4541: Standard Test Method for Pull-Off Strength of Coatings Using Portable Adhesion Testers. 4 ISO 13179-1 Implants for surgery-Plasma sprayed unalloyed titanium coatings on metallic surgical implants. ⁵ ASTM F1147: Standard test method for tension testing of calcium phosphate and metallic coatings. ⁶ ASTM C1499: Standard Test Method for Monotonic Equibiaxial Flexural Strength of Advanced Ceramics at Ambient Temperature.

Implant surface modification by a controlled biomimetic approach

A Carino¹, A Testino¹, E Mueller², M de Wild³, F Dalcanale³, P Gruner⁴, W Moser⁵, B Hoechst⁶

¹ Paul Scherrer Institut, ENE-LBK, Villigen, CH. ² Paul Scherrer Institut, BIO-EMF, Villigen, CH.

³ School of Life Sciences FHNW, Institute for Medical Engineering and Medical Informatics, Muttenz, CH. ⁴ Medicoat AG, Maegenwill, CH. ⁵ Atesos Medical AG, Aarau, CH. ⁶ Hager & Meisinger GmbH, Neuss, DE

INTRODUCTION: Titanium and its alloys are the most frequently used biocompatible materials in medical engineering. Accelerated osseointegration can be achieved by modifying the Ti surface with a layer of calcium phosphate (CaP). Current processes typically generate a relatively thick CaP (e.g., by plasma spray) and only a few thin coatings are available [1, 2]. We developed a cost-effective protocol for Ti surface modification with a thin CaP layer using a wet biomimetic route [3].

METHODS: A sand-blasted and acid-etched Ti grade 4 material is used as starting substrate. The surface topography is similar to that of commercially available dental implants. The novel surface treatments consist of two steps. In the first step (a modified version of the Kokubo method [4]), the formation of a highly porous layer of hydrogen sodium titanate ceramics is promoted. This layer is strongly joined to metal and renders the implant surface able to accelerate the formation of apatite (grafting layer, Figure 1A). In a second step, a thin layer of synthetic bone (CaP) is grown wet chemistry technique. physicochemical parameters which allow the controlled growth of the synthetic bone are means of calculated by an thermodynamic-kinetic model of the aqueous system [5]. The CaP deposition occurs in the porosity of the grafting layer and on top of it (Figure 1B). During the whole process pH, ionic strength, temperature, and saturation level of the system are controlled on-line and in-situ ensuring the steady state conditions and the reproducibility of the process. Therefore, careful control over thickness, chemical phase, and morphology of the deposited synthetic bone is achieved.

RESULTS: A thin bioactive synthetic bone layer on Ti implant surface is attained. The layer does not alter the roughness induced by blasting or acidetching and the implant surface results to be homogenously modified, regardless of its microand macroscopic shape. The synthetic bone layer is firmly grafted to the metal. Mechanical tests demonstrate that the modified surface is preserved upon implantation and the layer does not delaminate. The mechanic stability is obtained

thanks to the optimized metal-ceramic joining of the grafting layer, whereas the modified surface with synthetic bone offers an ideal substrate for natural bone growth after implantation.

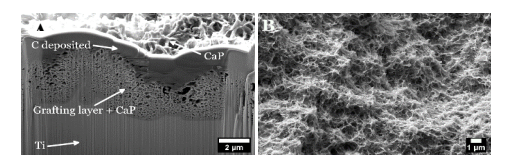


Fig. 1: Modified surfaces: (A) FIB cross-section; (B) surface after step 2.

Thanks to the control over the process, a <100 nm layer hydroxyapatite (HA) or octacalcium phosphate (OCP) can be deposited. In particular, OCP is considered the most bioactive CaP phase, being the precursor of natural bone in the osteogenesis. Reduced healing time and faster transition between primary and secondary stability of the implant can be expected. Moreover, the synthetic bone layer has a solubility higher than that of mature hydroxyapatite, which could promote remodelling to natural bone.

DISCUSSION & CONCLUSIONS: Ti implant prototypes with biomimetically modified surface have been produced and show promising chemical and mechanical in-vitro properties.

REFERENCES: ¹ Promimic AB, Sweden. www.promimic.com. ²L. M. Svanborg et al (2014) Evaluation of bone healing on sandblasted and Acid etched implants coated with nanocrystalline hydroxyapatite: an in vivo study in rabbit femur. International Journal of Dentistry 197581. ³ PCT/EP2018/076267. ⁴T. Kokubo et al (2010) Bioactive Ti Metal and its Alloys Prepared by Chemical Treatments: State-of-the-Art and Future Trends. Advanced Biomaterials 12:B597. 5 A. Carino et al (2018) Formation and transformation of calcium phosphate phases under biologically relevant conditions: Experiments and modelling. Acta Biomaterialia 74:478.

ACKNOWLEDGEMENTS: We thank the Swiss Nanoscience Institute and Medicoat AG for the financial support, and Hager & Meisinger for supplying the implants.

Development of an anodized titanium implant film with antimicrobial properties

<u>J Disegi¹</u>, S Williamson², M Roach²

Advanced Biomaterial Consulting LLC, Reading PA, USA.

INTRODUCTION: Anatase and rutile allotropic forms of titanium dioxide (TiO₂) demonstrate photocatalytic properties that have been shown to suppress bacterial activity [1]. A pulsed titanium anodization waveform was investigated in order to determine if a crystalline TiO₂ structure could be produced with antimicrobial properties.

METHODS: Test coupons consisted of 2.00 mm thick CP Ti Grade 4 sheet that met ASTM F67 standard. Coupons were cleaned, immersed in HNO₃-HF, and gold anodized in H₂SO₄ or neutral salt bath to provide amorphous TiO₂ controls. Four carbon counter electrodes and a copper bar were used for pulsed anodization trials. Two-theta X-Ray Diffraction (XRD) scans were performed between 23° - 30° at a continuous scan rate of 2° per minute. Surface morphology was evaluated via Zeiss Supra 40 SEM, Clemex image analysis, and Veeco Bioscope Catalyst AFM. Triplicate colonies of S. sanguinis (associated with dental infections) and Methicillin Resistant Staphylococcus Aureus (MRSA) were grown to logarithmic phase (108) colony forming units/ml) for exposure periods of 24 or 48 hours at 37 °C. Near-UV light activation was performed at 350-385 nm wavelength based on documented information. One-way ANOVA determined significant differences $(\alpha = 0.05)$ and post-hoc Tukey analysis separated significant groups.

RESULTS: Previous evaluations indicated 5.6 M H₂SO₄ maximized a gold anatase structure, 2.8 M H₂SO₄ maximized a dark green anatase structure, and neutral salt bath anodizing was ineffective. Dark green anodizing had the highest anatase and rutile peak intensities. A SEM micrograph of a dark green anodized sample is shown in Fig. 1.

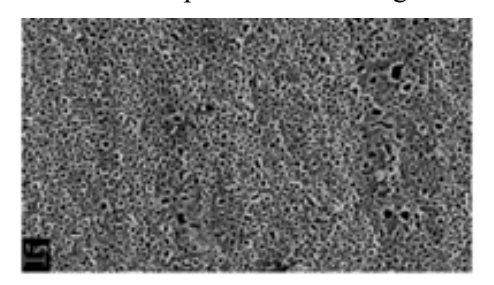


Fig. 1 SEM micrograph of dark green anodized sample with a 5% duty cycle (on-off time) in 2.8 M H_2SO_4 . (1 micron marker in lower left).

Triplicate pore measurements yielded 15.7 ± 0.6 % porosity, $10.7 \pm 0.9 \ \mu m^2$ density, and $138 \pm 5 \ nm$ mean diameter. MRSA antimicrobial activity is shown in Fig. 2.

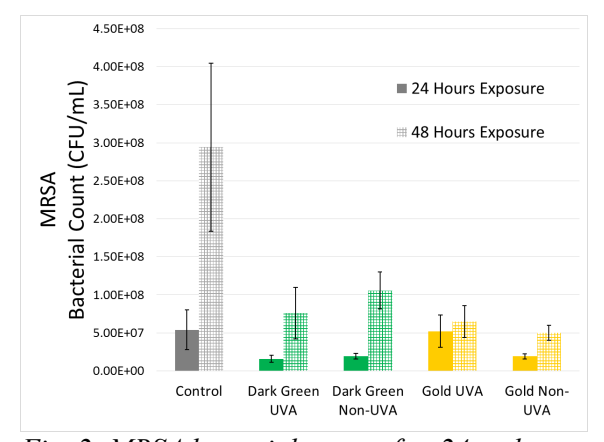


Fig. 2: MRSA bacterial count after 24 and 48 hours. All values represent significant differences versus control except for gold UVA at 24 hours.

DISCUSSION: Pulse anodization trials in H₂SO₄ produced dark green anodized TiO2 films that demonstrated statistically significant antimicrobial activity against S. sanguinis and MRSA. Near-UV light activation at 350-380 nm wavelength improved. S. sanguinis antimicrobial response but was inconclusive for MRSA. Other researchers [2] have shown that textured stainless steel reduced E.coli bacterial cells after 48 hours exposure. Photocatalytic TiO₂ response and nano surface features mav have both contributed antimicrobial activity. The nanometer surface film should improve osteoblast adhesion, durability, and adherence when compared to bulk coatings. Regulatory pathway should be straightforward since the TiO₂ surface contains no intentionally added substances.

REFERENCES: ¹L Visia et al (2011) Titanium oxide antibacterial surfaces in biomedical devices; *Int J Artif Organs* **34 (9)**:929-46. ² Y Jang et al (2018) Inhibition of Bacterial Adhesion on Nanotextured Stainless Steel 316L by Electrochemical Etching; *ACS Biomater Sci Eng* **4(1)**:90-7.

ACKNOWLEDGEMENTS: DePuy Synthes provided funding for this research project.

² University of Mississippi Medical Center, Jackson MS, USA

Protective coating for individual dental superstructures from CoCr alloy

<u>J Oranskiy</u>¹, <u>DV Tetyukhin</u>², <u>SA Molchanov</u>², <u>EN Kozlov</u>²

¹ <u>Dento-L-Master LLC</u>, Moscow, Russia. ² <u>CONMET LLC</u>, Moscow, Russia

INTRODUCTION: Presently, individually milled superstructures made from CoCr alloys are widely spread due to the availability of CAD/CAM technologies. However, CoCr alloy application has the following disadvantages: oxidation of metal surfaces that were not coated by dental ceramic during the sintering process under temperatures. The need for oxidized layer removal (e.g. by sandblasting treatment) leads to a change in shape and size of the superstructure interface and, consequently, increase of micro-mobility and hermeticity loss in the implant-abutment connection and emergence of a galvanic pair with titanium implants. Deposition of submicron nanocrystalline coating of Al₂O₃ with the thickness of 0.1 - 0.5 µm allowed to solve the issues.

METHODS: For coating individually milled superstructures an atomic layer deposition method (ALD) was applied. The method allows applying thin and conformal metal oxide coatings [1]. Aluminium oxide is chosen due to its high heat resistance, strength and bio-inertness. To confirm the protective properties, experiments were on CoCr samples performed of dental superstructures and its pre-mills with Al₂O₃ coatings with a thickness of 0.1 µm and 0.15 µm. To test the heat resistance, the samples were subjected to cyclic heating in an atmosphere according to the standard mode for facing CoCr alloy frame with ceramic masses. Then the samples were checked for the integrity and stability of the oxide layer. For assessing the barrier properties of the coating, its dielectrical strength was being determined. Spherical electrodes with a diameter of 4 mm were applied to the flat or cylindrical surface of coated samples. A constant voltage from the DC power supply was applied stepwise by 0.05 V to electrodes. The emergence of breakdown was determined by the appearance of a current in the circuit, which was limited to 0.001 A.

RESULTS: The created Al₂O₃ submicron coating with 0.15 μm thickness allowed to protect the surface of individual dental superstructures from thermal oxidation during the sintering process (5 cycles of heating up to 1000 °C (Fig. 1)), and to improve as well the barrier properties of the surface due to the high dielectrical strength of the coating (Table 1), significantly reducing the risk of the galvanic pair emergence.

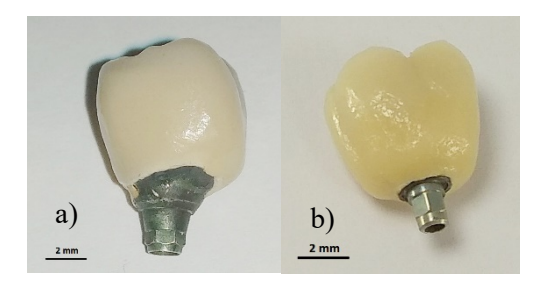


Fig. 1: Individual dental superstructures after 5 cycles of ceramic facing a) without the protective coating, b) with the protective coating.

Table 1. Dielectric strength of Al_2O_3 coatings on CoCr samples.

No	Description of samples	Coating thicknes	Breakdown voltage, V
	•	s, µm	O ,
1	Pre-mill with	0.1	0.775 ± 0.025
	coating		
2	Pre-mill with	0.15	2.45 ± 0.05
	coating		
3	Individual	0.15	2.45 ± 0.05
	superstructure		
	with coating and		
	ceramic facing		

DISCUSSION & **CONCLUSIONS:** The conducted studies confirm that the use of Al₂O₃ coating in the manufacturing process of superstructure produced from CoCr alloys excludes interface oxidation during the dental ceramic sintering process, as well as formation of dielectric barrier between the superstructure and a titanium implant. Taking into account innovativeness of the ALD-method it is necessary to conduct additional research. in vitro and in vivo studies.

REFERENCES: ¹ V. Miikkulainen, M. Leskelä, M. Ritala, and R. L. Puurunen (2013) Crystallinity of inorganic films grown by atomic layer deposition: Overview and general trends; *J. Appl. Phys.* **113**:021301.

Characterization of particulate contaminants and its challenges

S Rohrer¹, D Streit², F Bigolin², R Wirz¹, N Döbelin¹, M Bohner¹

¹Bioceramics & Biocompatibility Group, ²Materials Group, RMS Foundation, Bettlach, CH

INTRODUCTION: Manufacturers of medical devices are being requested by the FDA to indicate the level and type of particle contamination of their product and to evaluate the potential risk for the patients. As part of a 510(k) premarket approval submission, a client had to determine the particle contamination of the polymeric film component of its negative pressure wound therapy kit, and to compare it to that of a predicate device.

METHODS: Contaminant particles were extracted from the polymer films and from blanks in three different solvents at 50 °C, according to ISO 10993-12:2012 [1] and to special requirements of the FDA. The particles were then collected on a polyamide filter, counted and divided into non-metallic, fibres, and metal particles with an automatic filter analysis system of JOMESA (JOMESA HFD), and characterized by FTIR (Bruker LUMOS) or EDX (Zeiss Evo MA25). All experiments were done in triplicate.

RESULTS: The highest total number of particles determined per client or predicate device film was 516 and 1233, respectively. The highest number of $\geq 25~\mu m$ particles determined per client or predicate device film was 155 and 542, respectively. While the amounts of particles extracted from the client's films were always below the thresholds specified in the USP <788> standard (max. 300 \geq 25 μm particles and 3000 \geq 10 μm particles) [2], the amount of \geq 25 μm particles extracted from one predicate device film was above this threshold.

Overall, 16 types of particles were detected in the extracts of the client's films (e.g., a non-alloy steel particle shown in Fig. 1a). Comparing, 36 types of particles were detected in the extracts of the predicate device film and 20 types in the blank controls presumably due to residual particles from the clean room environment. Regardless of the extraction medium, the vast majority of the particles found were non-metallic particles. The most abundant contaminants in the extracts of the client's film were PU particles, cellulose fibers, CrNi steel particles, the antioxidant, cellulose, polyamide, and polypropylene particles. Except for the CrNi steel particles, all these particle types were also repeatedly observed in the extract of the predicate device films. However, these extracts

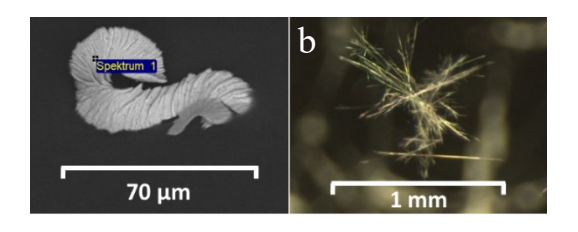


Fig. 1: Microscopy images of different particles — a) shows an unalloyed steel particle found in a water extract from the client's polymer film. b) shows a crystallized antioxidant found in all hexane extracts of polymer films.

additionally contained particles out of proteins (possibly skin residues), wool (animal derived), and nail polish.

The polymer films of the client and the predicate device showed partial decomposition in hexane and ethanol. Fine needles (Fig. 1b) precipitated during hexane cooling. These needles were identified as the antioxidant N,N'-Hexamethylenebis(3,5-di-tert-butyl-4-

hydroxyhydrocinnamamide), which is used in the raw material of the films. Extraction in 95 vol% ethanol resulted in the formation of fine white particles in the sediment, which were identified as polyurethane film base material.

DISCUSSION & CONCLUSIONS: Difficulties were encountered at different levels such as: (i) the design of the extraction experiments, (ii) the large size, surface area, and electrostatic behaviour of the film; (iii) the technical limitations of optical microscopy and FTIR chemical identification; (iv) the partial decomposition of the films in hexane and ethanol; (v) the contaminants present in our clean room; (vi) the statistical analysis. However, the results demonstrated that the client product contained fewer contaminant particles than the threshold values set in the standard USP < 788> and that their chemical compositions were unproblematic. Contrarily, a predicate device contained too many particular contaminants, and some were critical, such as nail polish and wool / proteins.

REFERENCES: ¹ ISO 10993-12:2012: Biol. evaluation of medical devices - Part 12: Sample preparation and reference materials. *International Organization for Standardization* (07-2012). ² USP <788>: Particulate Matter in Injections. *United States*

ACKNOWLEDGEMENTS: The authors would like to thank the client for the possibility to publish their case.

Pharmacopeia (01-07-2012).

Effect of Ti on the wear properties of CoCrMo-alloy: Investigations under fretting corrosion

K Maeda¹, S Nakahara¹, T Masanori¹, K Ueda¹, T Narushima¹, F Farizon², J Geringer³

¹ Dpt of Materials processing / Tohoku University, Japan. ² University Hospital of Saint-Etienne, CHU-COT, INSERM U1059, Saint-Etienne, France. ³ Health Engineering Center, Mines Saint-Etienne, INSERM U1059, Saint-Etienne, France

INTRODUCTION: corrosion Fretting phenomenon can lead to wear and corrosion of many contact surfaces found in a corrosive media. Fretting corrosion can occur in motors of cars, turbines, and sometimes this phenomenon can occur on some parts of the metallic surfaces of orthopaedic implants, thus resulting in wear particles release that can be deleterious for the patient's health. Decreasing the wearing of metals in vivo as a result of fretting is an important point to achieve, thereby decreasing the level of allergic reactions and immune responses to metallic wear particles in the human body. CoCrMo is an alloy which is widely used in industry for manufacturing of artificial joints.

METHODS: This study focuses on understanding the effect of 1 % Ti on the resistivity of CoCrMoalloy against wearing when subjected to fretting corrosion conditions. The fretting corrosion experiments were conducted with CoCrMo and CoCrMo with 1 % Ti alloys (Fig 1). The samples were subjected to fretting against different polymers such as PMMA (Polymethyl-methacrylate), PEKK (polyetherketoneketone), and PEKK with 30 % carbon fibres. The goal was to compare the wearing resistivity of the CoCrMo-alloy with and without 1 % Ti against different types of polymers. The duration of the experiment was 4 hours in 0.1 M + 30 g/L albumin solution and the displacement was 80 µm. In addition, 3D profilometric and SEM images were taken to characterize the shape of the worn zones on the surface of the metallic samples.

RESULTS: Wearing of CoCrMo was the highest against PMMA. On the other hand, CoCrMo showed lower wearing against PEKK and the lowest wearing was against PEKK with 30 % CF. As for CoCrMo with 1 % Ti, the wearing was lower against the 3 polymers compared to CoCrMo upon

fretting against PMMA, PEKK and PEKK with 30 % carbon fibres. The effect of 1 % Ti on CoCrMo alloys was a better resistance against fretting corrosion phenomenon.

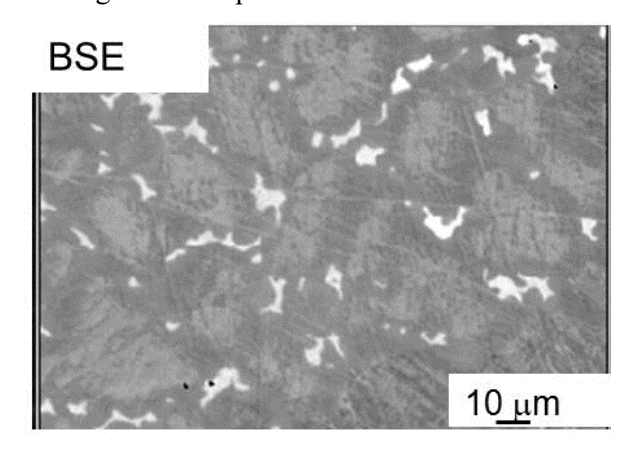


Fig. 1: Back Scattering Electron Image of the Co-28Cr-6Mo-0.25C-1Ti.

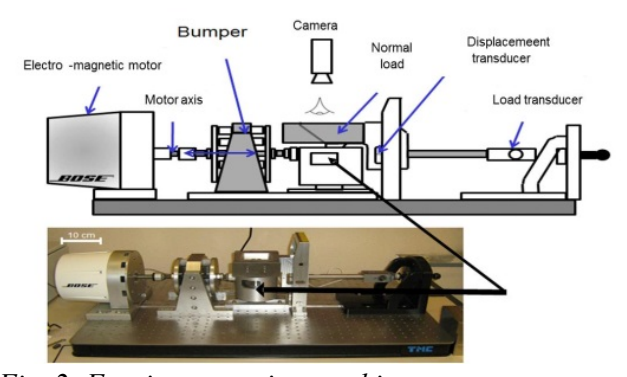


Fig. 2: Fretting corrosion machine

DISCUSSION & **CONCLUSIONS:** The CoCrMo-alloy with 1 % Ti might be a good candidate to decrease the wear under fretting corrosion conditions.

REFERENCES: ¹ K. Ueda, M. Kasamatsu, M. Tanno, K. Ueki, J. Geringer, T. Narushima (2016) *Materials Transactions* 57:2054-9.

Particles and ions generated in total hip joint prostheses: in vitro wear test results of UHMWPE and XLPE acetabular components

<u>H Zohdi</u>, B Andreatta, <u>R Heuberger</u> *RMS Foundation, Bettlach, CH*

INTRODUCTION: The accurate and detailed characterization of wear particles and ions released from total hip joint prostheses is essential to understand the cause and development of osteolysis, aseptic loosening and hypersensitivity.

METHODS: The wear particles and ion release of 22 different test liquids from hip simulator studies were investigated. Wear particles generated from acetabular components made of ultra-high-molecular-weight polyethylene (UHMWPE) or cross-linked polyethylene containing vitamin E (XLPE, all from Mathys Ltd. Bettlach, CH) were isolated by acidic digestion and characterised using scanning electron microscopy (SEM) and laser diffraction. Additionally, we investigated the effect of accelerated ageing, running-in versus steady-state, head materials and calcium sulphate third-body particles [1] on the morphology and size of the created debris.

The Fe, Ni, Mn, Nb, Co, Mo and Al ions released from femoral heads made of stainless steel, CoCrMo and alumina ceramic were analysed using inductively coupled plasma mass spectrometry (ICP-MS).

RESULTS: The wear particles were predominantly in the submicron range and of globular shape, with occasional fibrils (Fig. 1). The size distributions of the UHMWPE and XLPE particles were similar (Fig. 2); however, more fibrils were observed among the UHMWPE particles [2]. The average particle size decreased for most samples in the

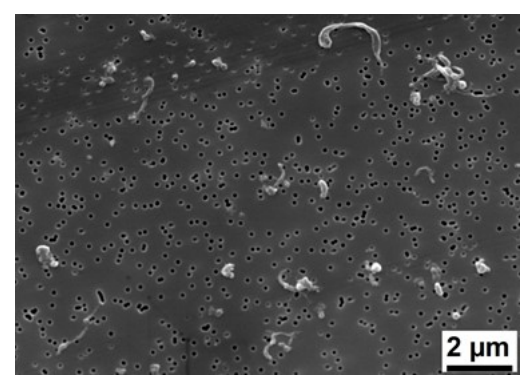


Fig. 1: SEM-image of globular wear particles and fibrils from an aged UHMWPE liner.

steady-state phase compared to the running-in. The

steady-state phase compared to the running-in. The accelerated ageing and the presence of third-body

particles generally caused larger UHMWPE wear particles only.

The ion concentrations were very low and close to the detection limit. However, increasing the size of the stainless steel femoral heads led to an increased ion level [2].

DISCUSSION & CONCLUSIONS: Although SEM is the most standardized technique to characterize the morphology of wear debris, it led to an over-estimation of the particle size (Fig. 2). However, the combination of SEM and laser diffraction was very powerful to analyse both the morphology and the particle-size distributions of the polyethylene wear particles.

Most particles were in the submicron range and globular, whereas the size distribution from UHMWPE and from XLPE particles were similar. Low concentrations of ions were released from the head materials.

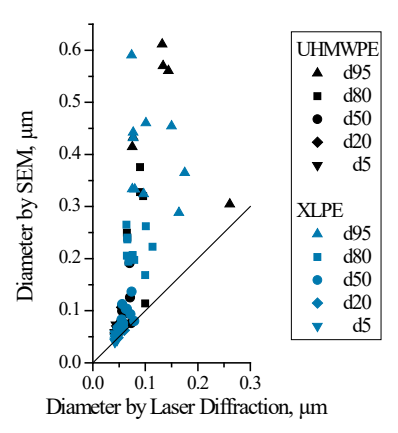


Fig. 2: Percentiles of the equivalent diameter of polyethylene particles determined with SEM vs. diameter determined using laser diffraction.

REFERENCES: ¹ R. Heuberger, P. Wahl, J. Krieg, E. Gautier (2014) *eCM* **28**:246. ² H. Zohdi, B. Andreatta, R. Heuberger (2017) *Tribol Lett* **65**:92.

ACKNOWLEDGEMENTS: We thank O. Loeffel and T. Imwinkelried (both RMS Foundation) for their help and the RMS Foundation for the financial support

Evaluation of gamma irradiation impact on 3D-printed multimaterial polymer

A Pfeil¹, F Schuler², L Barbé¹, F Geiskopf¹, M de Wild², P Renaud¹

INSA-ICUBE, Strasbourg, France. ² FHNW-HLS, Muttenz, CH

INTRODUCTION: Multimaterial additive manufacturing may offer new possibilities for design of medical devices thanks to the freedom of material. Rigid shape and and biocompatible materials are now available so polymer devices could benefit from the materials and the novel production process [1-2]. To this purpose, we investigate the impact on mechanical performance of γ-irradiation, a standard sterilization process, to polymer parts.

METHODS: Polyiet technology (Stratasys Ltd. USA) is being studied with a Connex 350 system processing UV-curing resins. A rigid material, commercialized as Verowhite Plus, and a flexible one, TangoBlack Plus, are assessed. Mechanical performance is tested using tensile tests according to ISO 527-1 for the rigid material, with type 1A specimen. For the flexible material, a sample is designed to have a length of reduced section of 25 mm, and a cross section of 4*4 mm². Five specimens of rigid materials and one of flexible material are tested, before and after irradiation at 34 kGy. In addition, an assembly of 3D-printed parts of both materials to build a pneumatic medical actuator [3] is tested in terms of biopsyneedle positioning velocity before and after irradiation.

RESULTS: The stress-strain curves of the rigid material are shown in Fig. 1. The Young's modulus (mean \pm std) of the unexposed and the γ -exposed specimens are equal to 1830 ± 38 MPa and 2810 ± 37 MPa, respectively. γ -irradiation has a significant stiffening effect. It is also to be noted that 2 out of 5 specimens show a rupture before 4.5% of strain. The other 3 specimens present a stress increase in the plastic domain that was not observed before irradiation. No significant impact is noted for the flexible material. The pneumatic actuator (Fig. 2) is still functional after irradiation despite the Young's modulus increase of rigid material, with no significant variation of velocity.

DISCUSSION & CONCLUSIONS: The 53 % increase of the Young's modulus and the stress-strain relationship of the rigid material could be explained by a reticulation of the polymer structure under gamma exposition. This work allows the designer to compensate the stiffening effect during design for additive manufacturing process. The

insignificant impact on flexible material and the satisfying behaviour of pneumatic actuators are encouraging to further test the materials and perform microbiological testing of γ -exposed materials.

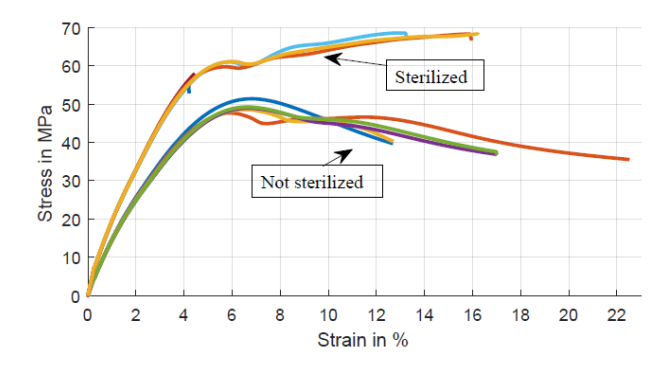


Fig. 1: Stress-strain curve of the rigid polymer specimens, before and after γ -sterilization.



Fig. 2: 3D printed multimaterial pneumatic medical biopsy actuator after gamma irradiation.

REFERENCES: ¹N. Nagarajan, A. Dupret-Bories, E. Karabulut, P. Zorlutuna, N.E. Vrana (2018) Enabling personalized implant and controllable biosystem development through 3D printing; *Biotechnology Advances* **36(2)**:521–33. ²A. Amelot, M. Colman, J.-E. Loret (2018) *The Spine Journal* **18(5)**:892–9. ³ A. Pfeil, L. Barbé, B. Wach, A. Bruyas, F. Geiskopf, M. Nierenberger, et al (2018) A 3D-Printed Needle Driver Based on Auxetic Structure and Inchworm Kinematics. *ASME IDETC* V05AT07A057.

ACKNOWLEDGEMENTS: The SPIRITS project is supported by the Region Grand Est, Land Baden-Württemberg, Land Rheinland-Pfalz, Cantons Baselstadt, Basellandschaft, Aargau, Swiss Confederation and by the program INTERREG Upper Rhine from the ERDF (European Regional Development Fund).

Cleanliness aspects of coated orthopaedic devices

B Dhanapal

Analytical Testing Services, Quality Assurance, EMEA, Zimmer Biomet, Winterthur, CH

INTRODUCTION: Cleaning orthopaedic implant devices commonly involves aqueous detergent based processes. The detergent solutions can be acidic, alkaline, neutral or enzymatic and ultrasonic may also be utilized. Typically, coated devices represent challenges for cleaning, as the cleaning process must remove manufacturing materials, processing aids, and other contaminations, but retain the coated surface unaffected. Ultrasonic cleaning removes not only the contaminations but also a part of the coating materials.

For Hydroxyapatite-coated (HA) devices, first of all it is essential that the raw material is in compliance to ASTM F1185 [1]. During coating, masking materials are used to cover areas of the implant that are not intended to receive surface treatments. The masking material residue shall be removed with an appropriate solvent.

Purified water based cleaning may be detrimental to HA-coated implants because HA is partly soluble in water and has high affinity to a broad range of contaminations. For instance bacterial endotoxins are adsorbed to the surface. Extraction according to ASTM F2459 [2] method accounts for polar and non-polar contaminations. An ultrasonic assisted process does not only remove contamination, but also parts of the coating material, which is intended to be present by design. This makes it challenging to use only gravimetric methods for residual analysis. Therefore it is essential to use or combine more specific analytical methods, such as ICP and HPLC as described in ASTM F2847 [3].

METHODS: In our approach, the test parts were assayed for extractable residues by Fourier Transform Infrared spectroscopy (FT-IR), for water extractable residues by Total Organic Carbon (TOC), and for water extractable insoluble particulate matter by gravimetric method.

RESULTS: Based on our experience using ASTM F2459 to quantify residuals gravimetrically, the typical detection limit (DL) for soluble residues of

0.3 mg/part is more than a factor ten (0.02 mg/part) higher than the FT-IR method described there. Lower DLs may be necessary to assure a reliable assessment of the cleanliness of certain products in a statistical manner.

DISCUSSION: There are challenges with respect to manufacture and quality control of coated devices. In this presentation we focus on manufacturing, cleaning and quality assurance of the device.

Although ASTM F2459 has made a significant contribution to the orthopaedic industry in regards to evaluating the cleanliness of 100 % metallic medical devices, more standardization is needed especially in the case of coated devices.

CONCLUSIONS: Relationship between biological evaluation, cleaning validation, and sterilization validation is illustrated in the ISO 19227 standard [4]. Control of critical in-process cleaning is essential in order to achieve clean coated devices according to ISO 19227. Cleaning validation can be declared complete only when the sterilization validation and the biological evaluation of the implants are completed in accordance to ISO 10993-1.

REFERENCES: ¹ ASTM F1185, Standard composition of hydroxyapatite. ² ASTM F2459, Standard test method for extracting residues from metallic medical components and quantifying via gravimetric analysis. ³ ASTM F2847, Standard practice for reporting and assessment of residues on single use Implants and single use sterile Instruments. ⁴ ISO19227 Implants for surgery, Cleanliness of orthopaedic implants – General Requirements.

ACKNOWLEDGEMENTS: Thanks to the active collaboration of ASTM F04, ISO/TC 150 and Zimmer Biomet colleagues.

Holographic identification of titanium implants

M de Wild¹, R Krähenbühl², D Kallweit², R Marek¹, M Estermann³, M Schnieper²

¹ <u>University of Applied Sciences Northwestern Switzerland</u>, School of Life Sciences, Muttenz, CH.

² <u>Centre Suisse d'Electronique et de Microtechnique CSEM</u>, Muttenz, CH.

³ Thommen Medical AG, Grenchen, CH

INTRODUCTION: An innovative design attribute was developed as Unique Device Identification (UDI) for medical devices [1]. Holographic security features and highly complex Diffractive Optical Elements (DOE, revealing images like QR codes, logos, article or lot numbers when illuminated by a laser, see Fig. 2) are integrated directly into the titanium implant material to ensure traceability or brand protection to prevent product counterfeiting. This nanostructured surface-labelling is fully tissue-compatible because the embossing process is based on a physical structuring of the implant surface without additives or coating. The underlying holographic nanostructures are resistant to all conventional sterilization methods.

METHODS: A structured, ultra-hard steel stamp was used to emboss the surface of titanium parts for holographic labelling. The visibility of the created holograms was investigated for different process parameters and the precise and detailed submicrometer structure of the embossed surface was qualified by SEM and AFM. Wear tests have been performed for up to 5'000 stamping cycles on a moving titanium plate to prevent the same spot from being repeatedly stamped.

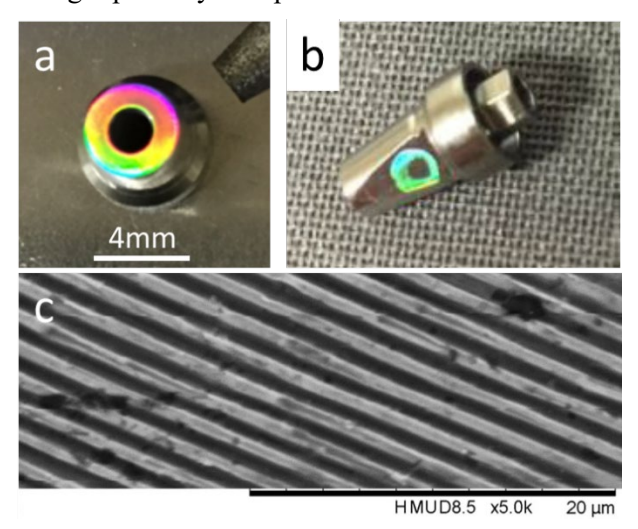


Fig. 1: a, b) Clearly visible embossed holograms on Ti abutments. c) Scanning Electron Microscopy image shows the periodicity of the diffractive structure on the tooled titanium surface.

RESULTS: The holographic structures can be transferred from the stamp to the surface of the titanium components. Diffractive characteristics

like iridescent light effect can be detected visually under white light (see Figures 1a and b) and the corresponding periodic pattern can be observed by SEM (Figure 1c). The most important process parameters identified were the temperature, the contact force per unit area and the surface roughness of the area to be stamped. With constant forming force, the embossing process becomes more efficient at higher process temperature and decreasing surface roughness of the stamping area.

The durability test of the stamp revealed a serviceability up to 5'000 tooling cycles. Although the average grating height of the master structure on the stamp was reduced by 32 %, the holographic effect is still nicely visible on the stamp and on the imprinted Ti devices. Even incompletely embossed patterns work as long as there is periodicity.



Fig. 2: A DOE-diffracted laser produces a visible, precalculated image on a screen.

DISCUSSION & CONCLUSIONS: It has been demonstrated that it is possible to transfer diffractive sub-micrometer structures such as visible holograms and Diffractive Optical Elements into titanium implant material. This unique holographic identification feature allows verification of the authenticity of implants, prosthetic parts or instrument and could serve as a UDI for medical devices.

REFERENCES: ¹ Unique Device Identification (UDI) for medical devices, Task Order No. 24, food and drug administration (2012).

ACKNOWLEDGEMENTS: This study was supported by InnoSuisse grant 18679.2 PFIW-IW.